IOP PUBLISHING JOURNAL OF MICROMECHANICS AND MICROENGINEERING

J. Micromech. Microeng. **18** (2008) 025006 (12pp) doi:10.1088/0960-1317/18/2/025006

Modelling and experimental analysis of the effects of tool wear, minimum chip thickness and micro tool geometry on the surface roughness in micro-end-milling

Hongtao Li[1], Xinmin Lai[1], Chengfeng Li[1], Jie Feng[2] and Jun Ni[2]

[1] State Key Laboratory of Mechanical System and Vibration, Shanghai Jiaotong University, Shanghai 200030, People's Republic of China
[2] Shien-Ming Wu Manufacturing Research Center, University of Michigan, MI 48109, USA

E-mail: xmlai@sjtu.edu.cn

Received 22 July 2007, in final form 8 October 2007
Published 21 December 2007
Online at stacks.iop.org/JMM/18/025006

Abstract

Tool wear, minimum chip thickness and micro tool geometry are found to have a significant influence on the surface roughness through experimental analysis of the micro-end-milling process. To address these issues, a surface roughness model is developed and validated in this present work. Firstly, experimental analysis for the tool wear and surface roughness was performed based on the micro-end-milling experiments of OFHC Copper by using 0.1 mm diameter micro endmills with a miniaturized machine tool. The cutting velocity and material removal volume are found to have a great effect on the tool wear, which will in turn affect the surface roughness significantly. Then, a trajectory-based surface roughness model for micro-end-milling is proposed and proven capable of capturing the minimum chip thickness, micro tool geometry and process parameters. Finally, based on this model, a surface roughness model with tool wear effect is developed by taking the material removal volume and cutting velocity into account and is experimentally validated. This model accurately predicts the surface roughness variation with tool wear progress and provides the means for further process design and optimization studies of the micro-end-milling process.

(Some figures in this article are in colour only in the electronic version)

1. Introduction

Miniaturized products with complex micro features manufactured in small volumes are increasingly in demand for various industries, such as aerospace, biomedical, defence and so on. Most of these components fall into the scale from 10 μm to 1 mm known as micro/meso scale in mechanical engineering. Considered as one of the most effective techniques, micro-end-milling can be used to fabricate these components with complex three-dimensional (3D) micro features over a wide range of material types. However, further advances in both the efficiency and the quality are limited by our incomplete understanding of the manufacturing process.

Surface roughness is a widely used index of product quality and in most cases a technical requirement for mechanical products. In addition, it also imposes one of the most critical constraints for production efficiency and process optimization. Although the surface roughness for conventional milling has been thoroughly investigated, the surface roughness in micro-end-milling is not yet fully understood. According to the studies of surface generation in conventional machining, many works demonstrated that the surface roughness could be calculated by tool geometry and processing conditions. Babin *et al* (1985) established a 3D surface roughness model by using the parametric tool path equations. Sutherland and Babin (1986) developed a geometry-based surface roughness model to investigate the

effects of the linear tool path and tool runout. It was concluded that the surface roughness was affected greatly by the feed rate and the tool geometry. However, the geometry-based approach is no longer accurate when it is applied to the micro-end-milling. Yuan *et al* (1996) investigated the effect of micro tool cutting edge radius on the surface roughness in the micro aluminium milling. It was found that larger cutting edge radius would increase the surface roughness due to the existence of the minimum chip thickness. Weule *et al* (2001) investigated surface generation in micro-end-milling of steel and concluded that the surface roughness had the increasing trend when the feed rate was smaller than the cutting edge radius. Vogler *et al* (2004) studied the floor surface roughness of micro-end-milling and attributed this phenomenon to the minimum chip thickness. These indicated that micro tool geometry and minimum chip thickness play an important role and should be considered in the surface roughness modelling of micro-end-milling.

Moreover, for the micro-end-milling process, the micro tool is one of the other most sensitive factors. Production efficiency, fabrication cost and surface quality are all related to the tool performance. Micro-end-milling utilizes the endmills typically with the diameter from 100 to 500 μm. Their ratio of worn volume to the portion of the tool getting involved in cutting is much larger than that of the conventional process, which surely induces great changes in the processing characteristics, including the surface roughness, milling forces, dynamic performances and so on.

However, very limited research on tool wear has been published due to experimental difficulties and the limited measurement technologies. Bao and Tansel (2000) studied micro tool wear using 1 mm diameter endmills. A milling force model was proposed to describe the tool wear effect from the experimental data, in which only the effect of material removal volume was considered. Rahman *et al* (2001) conducted pure copper micro milling experiments by using 1 mm diameter endmills. It was observed that the tool wear could be reduced by applying a larger depth of cut (DOC), and the tool wear in a lower cutting speed was much slower than that in a higher speed. Sinan *et al* (2007) performed experimental studies by using 0.2 mm diameter endmills. It was concluded that the tool wear had very little effect on the milling forces and surface roughness. In their experiments, tool wear was examined by forty 20 mm channels full slot cutting of OFHC Copper. However, this machining quantity is not enough for capturing tool wear features over the entire tool life span according to our experiments. Therefore, systematic parametric studies are necessary for understanding the tool wear effect in micro-end-milling. For conventional milling studies, many researches on the tool wear have been carried out. Medicus *et al* (2001) investigated the effect of tool wear on the milling forces and surface roughness in high speed machining of aluminium alloy. It was found that the cutting velocity had great influence on the tool wear. The higher the cutting speed, the more rapid the tool wears, which in turn increases cutting forces and surface roughness. Jawaid *et al* (2000) drew a similar conclusion in titanium alloy milling. Tony *et al* (1992) also found that the cutting velocity was the most significant factor for tool wear, while the feed rate had very little influence. Colding (2004) studied tool wear from a large number of experiments and found that there was a nearly exponential relation between the surface roughness and the material removal volume. All this research could be a valuable reference for micro-end-milling studies.

The goal of this paper is to study the effects of tool wear, minimum chip thickness and micro tool geometry on the surface roughness in micro-end-milling. Firstly, the experimental analysis of the tool wear and its effect on the surface roughness were conducted from systematically designed experiments, based on which the guideline for the surface roughness model is established. Then, a trajectory-based surface roughness model is built considering the minimum chip thickness, micro tool geometry and feed rate. Finally, a model with the effect of tool wear is developed and proven accurate by micro-end-milling experiments.

2. Micro-end-milling experiments

The experimental investigations presented in this study were done in the Shien-Ming Wu Manufacturing Research Center at the University of Michigan. A miniaturized machine tool (mMT) was developed for the micro-end-milling experiments. The work material is Oxygen-Free High Conductivity (OFHC) Copper Type 101, which is widely used in the optics, laser and microelectronics field. All the experiments were conducted by 0.1 mm diameter, two flute tungsten carbide micro endmills with a helix angle of approximately 30°.

In addition, dry milling was applied for all the experiments. The main considerations are from several aspects: (1) the work materials might be non-traditional mechanical materials for some applications of micro-end-milling and perhaps not suitable for lubricators. (2) Micro scale manufacturing is a high precision process, which usually has requirements of an extremely high standard for the environment. (3) The experimental data would not be comparable due to the differences in the properties of the lubricators.

2.1. Experimental set-up

The developed miniaturized machine tool is shown in figure 1. It is composed of three positioning slides: the motion controller, the spindle, the micro endmills and the milling forces dynamometer. The overall volume of the machine tool is $220 \times 190 \times 290\ \text{mm}^3$, and the working volume is $50 \times 50 \times 25\ \text{mm}^3$. Three dc motor stages with 0.1 μm resolution are used for precise positioning in the *XYZ* directions. Due to the reduced tool diameter, high rotation speeds of the spindle are required in order to obtain an adequate milling surface speed. An electrical NSK spindle ASTRO-E 800Z with a maximal rotation speed of 80 000 r min^{-1} and runout less than 2 μm is used. The milling forces are measured by a Kistler dynamometer 9256 C1 with a 2 mN threshold, and a natural frequency of 5.1 kHz, 5.5 kHz and 5.6 kHz in the *X*, *Y* and *Z* directions, respectively. The dynamometer is attached to a National Instrument Data Acquisitioning Board.

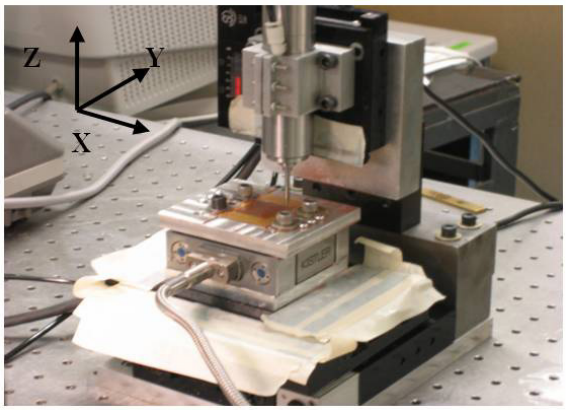

Figure 1. The miniaturized machine tool.

2.2. Process monitoring and surface roughness measurements

Due to the small dimensions of the micro tool, it is extremely difficult to monitor the milling process. In our study, the rotation speeds of the spindle are from 20 000 r min^{-1} to 70 000 r min^{-1}, with responding frequencies of the milling forces from 667 Hz to 2334.5 Hz. According to the sampling principle, a dynamometer with natural frequency of about 5 kHz could satisfy the requirements of the milling forces signals. The milling forces were sampled by the force dynamometer at a frequency of 10 kHz during the experiments and used for the purpose of online monitoring.

The micro channels produced with a width of 0.1 mm, which is equal to the diameter of the tool, make it a challenging task for the precise measurement of the surface roughness of the floor surface. A white light interferometer, Wyko NT2000, is used for the measurement of the floor surface roughness. It utilizes phase shift interferometry technology to realize sub nanometre resolution in the vertical direction. After each test, the floor surface of each channel was measured. A 606 μm $\times$ 460 μm area was sampled with 825.35 nm and 958 nm resolution in the feed and normal to feed direction with a 10.2$\times$ optical lens.

In addition, a Hitachi S-4700 scanning electron microscope (SEM) was used to examine the tool wear and the surface profile of the produced micro channels.

3. Experimental analysis of tool wear

3.1. Experimental design

One of the barriers for tool wear studies of micro-end-milling is the measurement technology and the criterion for the estimation of the micro tool wear. Due to the small dimensions of micro tools, it is extremely difficult to obtain the precise wear geometry, for example, the frank wear is usually used as the main criterion in the conventional milling process. In this study, the surface roughness is chosen to be the criterion for tool wear in micro-end-milling. Parametric studies for the tool wear were carried out from the analysis of the surface roughness experimental data. To perform experimental analysis of the tool wear and investigate its effect on the surface roughness, extensive experiments were conducted under the conditions listed in table 1.

Table 1. Process parameters for micro tool wear investigation experiments.

	RPM (r min^{-1})	V-stage (mm min^{-1})	DOC (μm)
1	20 000	48	10
2	40 000	48	10
3	70 000	48	10
4	20 000	80	6
5	20 000	24	20
6	70 000	80	6
7	70 000	24	20

The experiments were designed for experimental analysis of the effect of the tool wear on the surface roughness. Test nos 1, 2 and 3 were utilized to examine the effect of the cutting velocity. The rotation speeds of the spindle were chosen to be 20 000 r min^{-1}, 40 000 r min^{-1} and 70 000 r min^{-1}, respectively. Test nos 4, 5, 6 and 7 were designed to investigate the effect of the DOC and the feed per tooth (f_t). The DOC was chosen to be 6 μm and 20 μm, and the speed of the stage was chosen to be 80 mm min^{-1} and 24 mm min^{-1}.

In order to capture the complete progress of tool wear over the tool life span, for each test, a new tool was used for each test and kept machining until the tool was broken. The dimensions of the machined channel were 20 mm $\times$ 0.1 mm with a pitch between the slots of 200 μm. The depth of the slots was equal to the DOC of the tests. The milling forces were sampled by the dynamometer during the experiments and the floor surface roughness of each slot was measured by using the Wyko surface profiler after the experiments. Through these measurements, the surface roughness variations over the entire tool life were recorded for each test. Moreover, in order to avoid differences in the tool performances, the tools used were ordered from the same production batch.

3.2. Tool wear patterns

In order to investigate the tool wear procedures during micro-end-milling, many measurements were conducted to examine the tool geometry in the presence of severe wear. Due to the small tool dimension, SEM is utilized to check the tool wear geometry as shown in figure 2.

Figure 2(*a*) shows the image of the new tool with a diameter of 100 μm. Figures 2(*b*) and (*c*) show the images of the tool when severe wear occurs. It is observed that the main pattern of the tool wear is frank wear. From the measurement of figure 2(*c*), it is found that the worn geometry has a little asymmetry. Figure 2(*d*) shows the side view of the worn tool, it is observed that the tool wear is not uniform along the cutting edge, with the wear on the top portion a little larger. This kind of complicated wear will cause variation in the tool geometry, and will in turn result in an increase of the surface roughness.

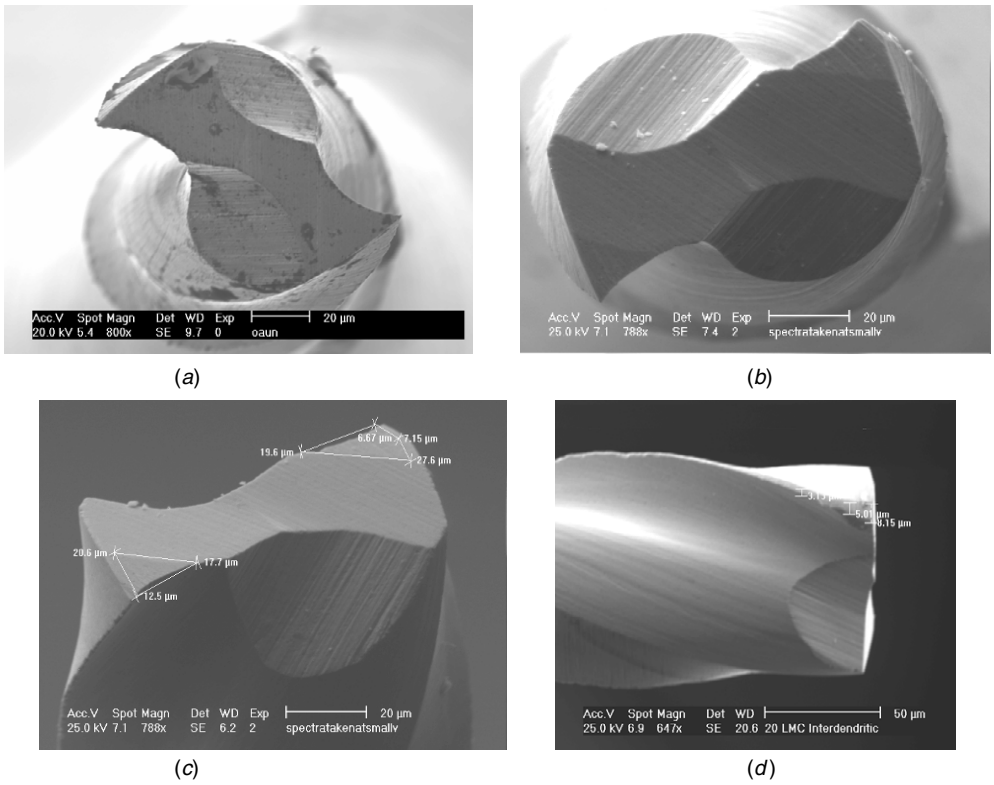

Figure 2. SEM pictures of the micro endmill (new tool and worn tool): (*a*) new tool, (*b*) worn tool (top view), (*c*) worn tool (main view) and (*d*) worn tool (side view).

In order to investigate the tool wear process, firstly, the average reduction in the tool radius, w, which represents the changes in the micro tool geometry caused by tool wear was examined. As shown in figure 3(*a*), w is calculated by

$$w = \frac{d_0 - d_{\text{wear}}}{2} \tag{1}$$

where d_0 is the diameter of the new tool, while d_{wear} is the diameter when the tool wear occurs. Since the diameter of the tool is very difficult to measure, especially for online processing, the widths of the machined channels were utilized as a measure of the tool wear (Sinan *et al* 2007). Therefore, d_0 can be obtained as the width of the channel at the beginning of the experiment, while d_{wear} is the width of the channel when the tool wear occurs.

The experimental data of the reduction in the tool radius, w, are plotted in figure 3(*b*). It is observed that w changed greatly from zero to the maximum $w_{\max}$ of about 10 μm with the tool wear progress, which means the tool was worn out for about 20 μm on its diameter. The procedures of the surface roughness variation have a similar trend with a typical tool wear process, which consists of three periods: first the tool wear develops quickly, then it goes into a relatively stable period and finally it progresses rapidly until it is broken.

w under different processing conditions was also examined as shown in figures 3(*c*) and (*d*). From these results, it is difficult to perform the parametric studies to determine the main factors influencing the tool wear process. Tool wear is a complicated process, and a micro tool with a diameter of only 0.1 mm induces many random factors. Although the reduction in the tool radius could simply represent the changes of the tool geometry when tool wear occurs, its effects cannot be described in such a simple way due to its complicated geometry as can be seen from the SEM picture.

On the other hand, through the surface roughness measurements of the machined channels, the changes were found to be more sensitive to tool wear and more reasonable for tool wear investigation. To some extent, this kind of variation could be considered as a comprehensive representation of the tool wear. In this study, it is chosen as the criterion for the evaluation of the tool wear effect.

3.3. Surface roughness experimental results and evaluation criteria

The sampled 3D surface profiles for the slots in test no 4, with a spindle rotation speed of 20 000 r min^{-1}, a DOC of 6 μm and f_t of 2 μm, are shown in figure 4. Figures 4(*a*)–(*c*) represent the surface topographies of the 3rd, 45th and 90th channels, respectively. From the figures, it is obvious that the surface quality changes greatly with tool wear progress. The Ra values for the entire floor surface are 144 nm, 196 nm and 535 nm, respectively. It confirms the necessity for consideration of the tool wear effect for the modelling of surface roughness in the micro-end-milling process.

Before the experimental analysis, the criterion for surface roughness evaluation needs to be determined due to the complicated surface characteristics when the tool wear occurs. As for the conventional milling process, the surface roughness along the central line of the floor surface is used to evaluate

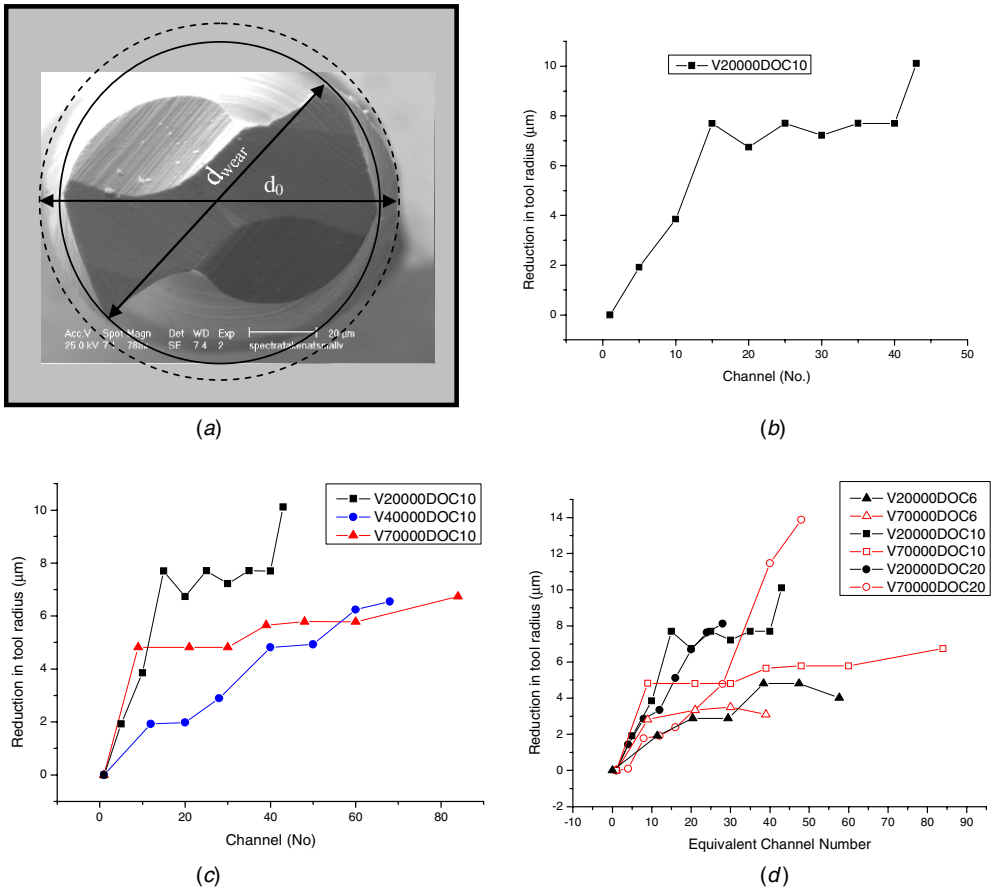

Figure 3. Tool wear in the micro-end-milling process: (*a*) tool wear length calculation, (*b*) w when $V = 20\,000$ rpm and DOC $= 10$ μm, (*c*) w at different cutting velocities and (*d*) w at different DOCs.

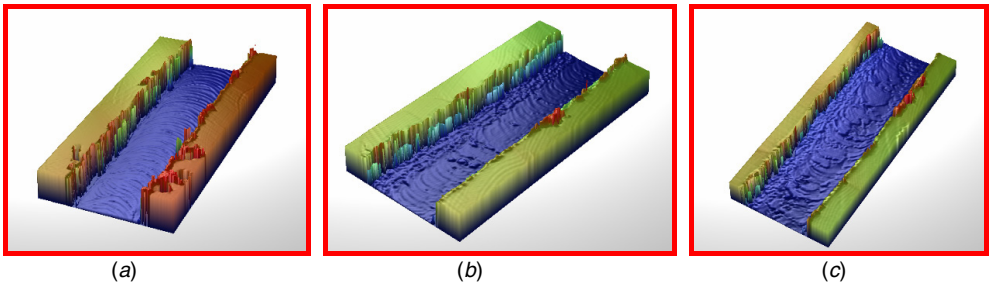

Figure 4. Surface topography of the channels (test no 4): (*a*) 3rd channel, (*b*) 45th channel and (*c*) 90th channel.

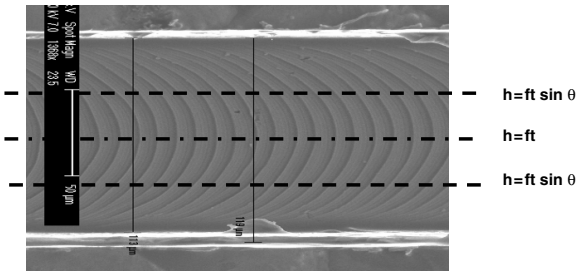

Figure 5. Tool trajectories on the floor surface of the machined slot.

the surface quality since the feed rate is greatest when the tool cuts pass the central line, as shown in figure 5, which will lead to the largest surface roughness along this line. This criterion is reasonable for the conditions when the tool is in good condition to make sure that the greatest feed rate is along the central line.

However, the situations are totally different when tool wear occurs. The SEM pictures of the surface generation are shown in figure 6, in which (*a*)–(*c*) represent the surface topographies of the 3rd, 45th and 90th channels, respectively. From figures 6(*b*) and (*c*), we can see that the tool path is not clear any more when the tool wears, and the surface profile corresponds to the tool wear geometry of the micro tool shown in figures 2(*b*) and (*c*). The surface roughness along the central line is no longer capable of representing the characters of the entire floor surface. Therefore, we take the

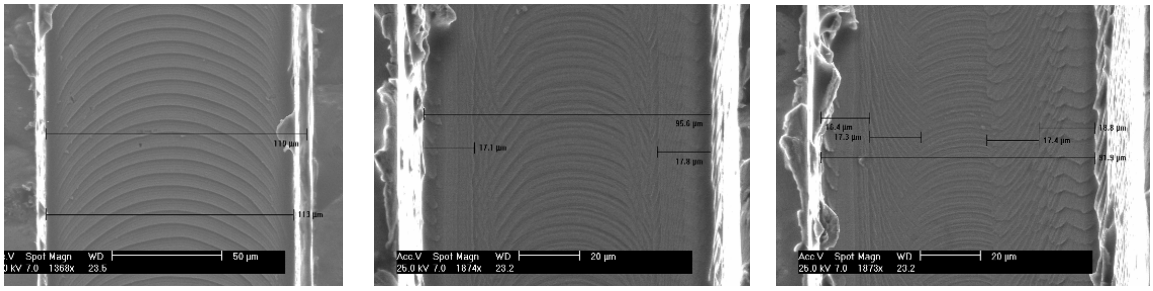

(*a*) (*b*) (*c*)

Figure 6. SEM pictures of the floor surface of the channels: (*a*) 3rd channel, (*b*) 45th channel and (*c*) 90th channel.

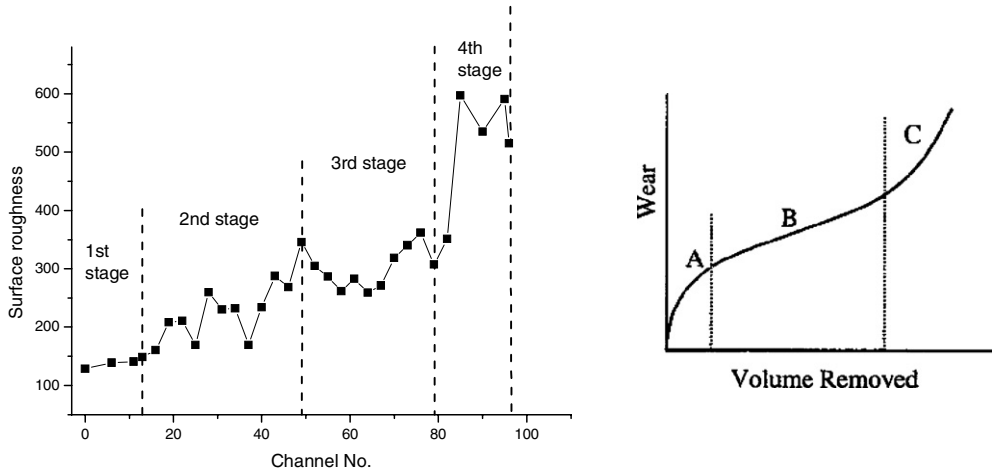

(*a*) (*b*)

Figure 7. Surface roughness with the tool wear progress: (*a*) experimental results of Ra (test no 4) and (*b*) typical tool wear curve.

surface roughness of the whole floor surface as the criterion when the tool wears.

From the above discussion, the surface roughness could be divided into two categories in micro-end-milling: one is the surface roughness at the start stage of the experiments when the micro tool is in good status. On these occasions, the surface roughness along the centric line of the floor surface is chosen to be the criterion for the surface roughness. This kind of surface roughness can be accurately calculated by the trajectory-based approach. The other is the surface roughness when the tool wear occurs. On these occasions, the surface roughness of the whole floor surface is taken as the evaluation criterion for the surface quality. Both of these two kinds of surface roughness can be obtained from the sampling data by the Wyko system.

3.4. Parametric studies of the tool wear

For the tool wear studies, we take test no 4 as the example to investigate the effect of the material removal volume on the surface roughness. The experimental data of the surface roughness are plotted in figure 7(*a*). It is observed that the surface roughness changed greatly from Ra at the start stage being about 128.5 nm to the maximum of 597.3 nm with tool wear progress. From the analysis of the Ra values, the variation of the surface roughness can be divided into four stages, as shown in the figure. In the first stage, the Ra value generally does not change much, which means that the tool does not wear during this period. In the second stage, the Ra value increases rapidly from 148.75 nm to 345.84 nm, which illuminates how the tool wear starts and progresses rapidly over this period. In the third stage, the Ra value fluctuates between 260 nm and 345.85 nm without obvious increase, which illuminates how the status of the tool was in a relatively stable stage during this period. In the fourth stage, the Ra value increases dramatically to 597.3 nm, which means the tool wears very quickly during this period. The procedures of surface roughness variation have a similar trend with typical tool wear process, shown as figure 7(*b*). This also confirms the speculation to use surface roughness as the criterion to study tool wear in micro-end-milling.

The results of the experiments designed for tool wear investigation are shown in figure 8. Figure 8(*a*) shows the dependence of the surface roughness on the material removal volume at different cutting velocities. The DOCs were all 10 μm. For each test, a similar trend with test no 4, increases in the surface roughness with tool wear progress, is clearly observed. By the comparison of Ra at different cutting speeds, it is found that the cutting speed has a great effect on Ra variation. For test no 3 with a spindle speed of 70 000 r min^{-1}, the Ra values increase from 153.4 nm to 2.41 μm, with the variation magnitude much larger than that of other tests with spindle speeds of 20 000 r min^{-1} and 40 000 r min^{-1}. Ra of 2.41 μm illuminates how the tool wear

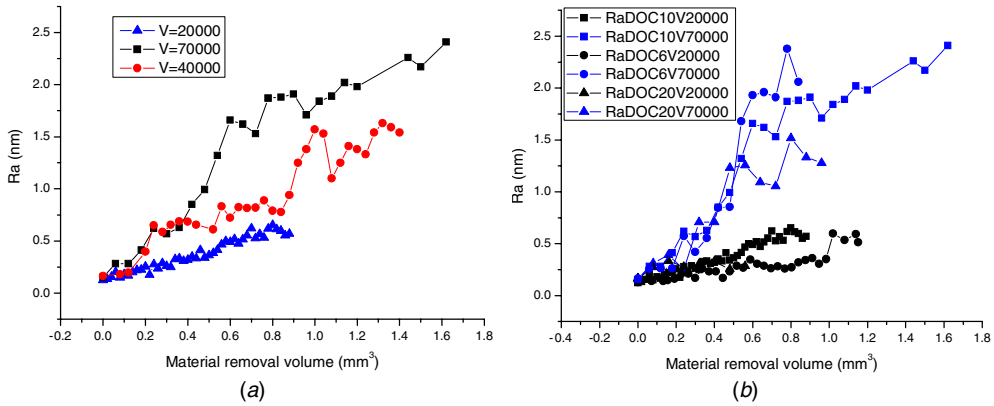

Figure 8. Surface roughness at different cutting conditions: (*a*) Ra at different cutting velocities and (*b*) Ra at different DOCs.

was quite severe before the tool was broken. Figure 8(*b*) shows the variation of Ra values at different DOCs when the spindle speed is 20 000 r min^{-1} and 70 000 r min^{-1}, respectively. It is clear that the variations in Ra are very close at different DOCs when the spindle speed is the same. In addition, for these tests at the same spindle speed, f_t was also different due to the different velocity of the stage. It demonstrates that the DOC and f_t have very little effect on the surface roughness variation.

3.5. Guideline of the surface roughness modelling

From the parametric studies, the main factors that influence the tool wear are found to be material removal volume and cutting velocity, similar to research on the conventional process (Medicus *et al* 2001, Jawaid *et al* 2000, Tony *et al* 1992 and Colding 2004). According to these analyses, the guideline of the surface roughness model is proposed as follows:

$$\mathrm{R}_a = K_{\mathrm{Ra}} \cdot \mathrm{R}_{a0} \tag{2}$$

$$\mathrm{R}_{a0} = \mathrm{R}_{a0}(f_t, h_{\min}, r_e) \tag{3}$$

$$K_{\mathrm{Ra}} = C_{\mathrm{Ra}} \cdot V^{m_{\mathrm{Ra}}} \cdot MR^{n_{\mathrm{Ra}}}. \tag{4}$$

As shown in equation (2), Ra_0 represents the surface roughness at the beginning of the experiments when tool wear does not occur. The increase in the surface roughness, which is due to the tool wear effect, is modelled by the coefficient K_{Ra}. With respect to the fact that K_{Ra} is related to tool wear, the main factors that mainly affect the tool wear are taken as the variables for the modelling of K_{Ra}. Therefore, the model includes two parts: the first is the model without considering the tool wear Ra_0, which represents the surface roughness when the tool wear is so slight that it could be ignored. The surface roughness does not change too much over this period. Ra_0 is modelled by a trajectory-based approach considering the minimum chip thickness, tool geometry and feed rate, shown as equation (3). The second part is the surface degradation model K_{Ra}, which is proposed to represent the increases of the surface roughness with the tool wear progress. The exponential relation is used according to the well-known Taylor model as equation (4), where C_{Ra}, m_{Ra}, n_{Ra} are the coefficients and can be calibrated from the experimental data. Next, the surface roughness modelling will be presented in detail.

4. A trajectory-based surface roughness model for micro-end-milling

This section focuses on the modelling and validation of Ra_0 in equation (3). The trajectory-based approach is applied to model the surface generation along the centreline in the full slot milling considering the minimum chip thickness, micro tool geometry and processing conditions. First, a surface roughness model for the conventional milling process is developed; then, the minimum chip thickness is estimated by FE simulations with respect to its significant effect on the surface generation of micro-end-milling; finally, a modification is made for the model to account for minimum chip thickness.

4.1. Surface roughness modelling for the conventional process

The schematic diagrams for the procedures of surface generation are shown in figure 9. Figure 9(*a*) shows the complicated 3D milling process; figure 9(*b*) shows a simplified diagram for the 2D process along the centric line of the floor surface; figure 9(*c*) represents the tool geometry of the tool nose radius by a close-up view of the tool tip; figure 9(*d*) plots the tool edge trajectories along the centre of the floor surface during the milling process with tool engagements in the feed direction. In the conventional process, the material that is in contact with the cutting edge is considered to be completely removed. Therefore, the surface generated is the interaction portion of the tool trajectories and can be predicted geometrically to a very high accuracy.

The tool geometry is defined by

$$y_{t0}(x) = \begin{cases} -\sqrt{r_c^2 - x^2} & \text{when} \quad x > -r_c \sin(\gamma) \\ -r_c \cos(\gamma) - [x + r_c \sin(\gamma)] \cdot \tan(\gamma) & \\ \quad \text{when} \quad x \leqslant -r_c \sin(\gamma) & \end{cases} \tag{5}$$

where x, y are the x and y coordinates, respectively, as shown in figure 9(*c*), r_c is the nose radius of the micro tool and γ is the angle as shown in figure 9(*c*). Therefore, the surface texture generated by the conventional milling process could be calculated by the geometry-based approach. The surface profile is shown as the hatched portion in figure 10(*a*).

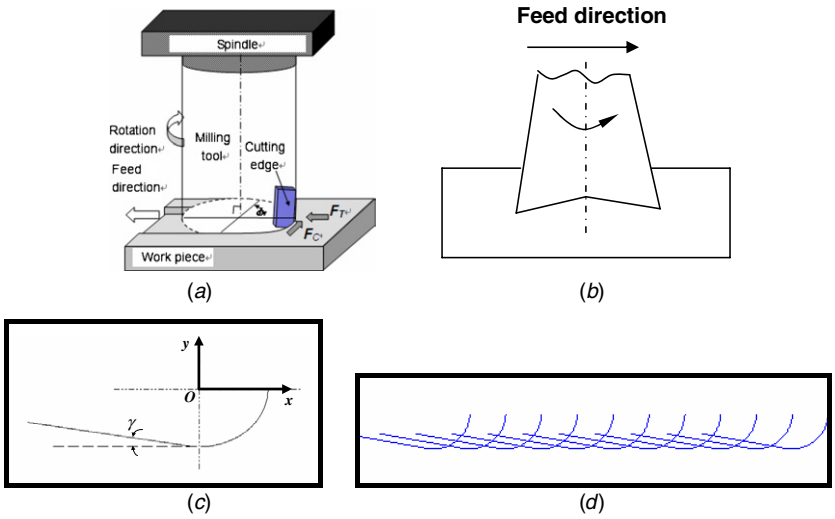

Figure 9. Schematic diagrams of the floor surface generation of the milling process: (*a*) milling process, (*b*) simplified 2D process, (*c*) tool geometry and (*d*) trajectories of the tool path.

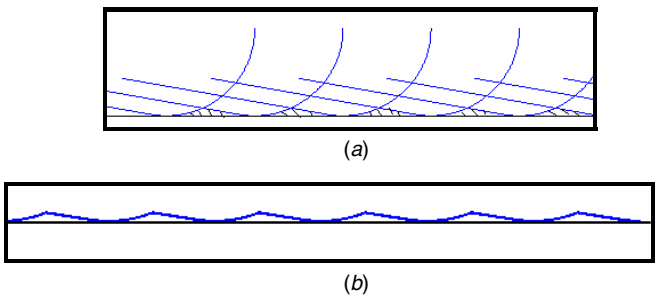

Figure 10. Surface generation in the conventional milling process: (*a*) trajectories of the tool path and (*b*) the generated surface profile.

The points formed the surface and could be picked up as figure 10(*b*), which can be used to compute the average surface roughness Ra. The software Matlab is utilized for the modelling of this approach and the computation of the surface roughness.

With respect to the fact that the tool nose radius of a micro cutter is one of the most significant parameters in this model, prior to the experiments, the 0.1 mm diameter micro endmill was imaged by SEM and the nose radius was estimated to be about 2 μm.

This geometry-based surface roughness model is capable of capturing the processing conditions and tool nose radius. For the conventional milling process, the main parameter that determines the Ra value is the feed rate f_t once the tool geometry is given. It is accepted that the surface roughness is approximately proportional to the square of the feed rate. However, as discussed above, the minimum chip thickness ($h_{\min}$) is another dominant factor that affects the surface roughness for the micro milling process. Therefore, a modification is needed to capture its effect.

4.2. Estimation of the minimum chip thickness

The minimum chip thickness is one of the key features for micro-end-milling and has an essential influence on the surface generation and the milling forces. Due to the existence of the cutting edge radius, the cutting process is driven by two mechanisms: the ploughing mechanism and the shearing mechanism. Transaction between the two mechanisms corresponds to the minimum chip thickness, $h_{\min}$, below which the chip is not formed. The minimum chip thickness, $h_{\min}$, is the function of the tool sharpness and the material properties.

Due to its essential role in micro-end-milling, the minimum chip thickness was investigated through FE simulations prior to being formulated into the surface roughness model. The FE model developed by Lai *et al* (2008) to study the influences of the size effect of the material behaviours at the micron level and tool cutting edge radius on micro-end-milling was used to determine the minimum chip thickness. The model is capable of analysing the size effect and the chip formation of the micro/meso scale machining process.

Simulation results are shown in figure 11. The uncut chip thickness t_c for the micro scale orthogonal machining was selected to be 0.1R (0.2 μm), 0.2R (0.4 μm) and 0.3R (0.6 μm). It can be clearly seen that there is no chip formed when h is 0.1R and 0.2R, while a chip forms when h is 0.3R. From these results, $h_{\min}$ is proposed to be 0.25R (0.5 μm) for OFHC Copper when the cutter edge radius is 2 μm and the rake angle is 10°. The results are consistent with some research. For example, Vogler *et al* (2003) estimated that the minimum chip thickness to edge radius ratios of pearlite and ferrite to be 0.20 and 0.3, respectively. Kim *et al* (2004) proposed that the minimum chip thickness be 30% of the cutting edge radius by means of MD simulations and experiments.

4.3. Modelling of the surface roughness considering the minimum chip thickness

With the geometry-based surface roughness model and the information of the minimum chip thickness, a modification

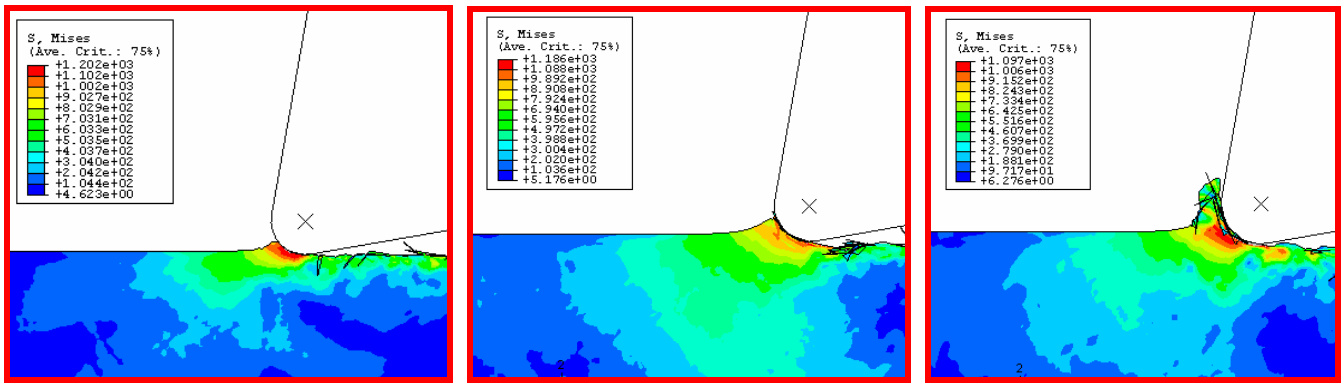

(*a*) (*b*) (*c*)

Figure 11. Chip formation in micro/meso scale machining: (*a*) $t_c = 0.1R$ (0.2 μm), (*b*) $t_c = 0.2R$ (0.4 μm) and (*c*) $t_c = 0.3R$ (0.6 μm).

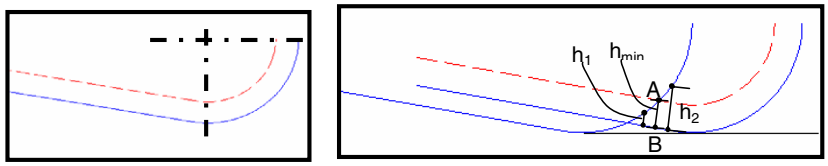

(*a*) (*b*)

Figure 12. Schematic diagram of the surface generation considering $h_{\min}$: (*a*) tool geometry and the $h_{\min}$ boundary and (*b*) algorithm for the update of the surface profile.

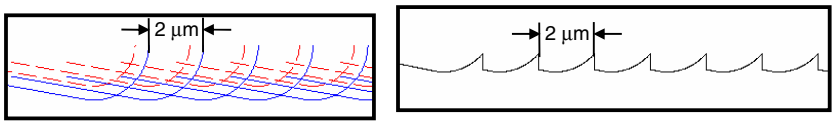

(*a*) (*b*)

Figure 13. Schematic diagram of the surface generation when $f_t \geqslant h_{\min}$: (*a*) trajectories of the tool path and $h_{\min}$ and (*b*) the generated surface profile.

is made to the conventional model with the minimum chip thickness concept. As shown in figure 12(*a*), a critical bound for $h_{\min}$, similar to the approach proposed by Vogler *et al* (2004), is defined by equation (6), with the distance between the tool edge and the bound of the $h_{\min}$ value (0.5 μm) shown as the dashed line. The surface profile modification is not based on the tool edge geometry but the critical $h_{\min}$ bound:

$$y_{h_{\min}}(x) = \begin{cases} -\sqrt{(r_c - h_{\min})^2 - x^2} & \text{when} \quad x > -(r_c - h_{\min})\sin(\gamma) \\ -(r_c - h_{\min})\cos(\gamma) - [x + (r_c - h_{\min})\sin(\gamma)] \cdot \tan(\gamma) & \\ \quad \text{when} \quad x \leqslant -(r_c - h_{\min})\sin(\gamma). & \end{cases} \tag{6}$$

When there is an engagement of the tool along the central line of the floor as shown in figure 12(*b*), the update computation of the surface profile can be divided into three steps. Firstly, the interaction point A between the tool geometry of the first pass and the $h_{\min}$ bound of the second pass is calculated for the surface profile update. Its corresponding point B on the tool geometry of the second pass was also recorded as clearly shown in figure 12(*b*). Then, the distance of the corresponding points between the tool edge geometry of the first and the second pass, h, is calculated in each engagement. Here, h represents the chip load of the milling process. The last step is the calculation of the surface profile update according to the concept of the minimum chip thickness. There are two different situations: one is that h is less than $h_{\min}$, as h_1 in figure 12(*b*), the surface profile is not modified since no chip forms in this portion. The other is that h is larger than $h_{\min}$, as h_2 in figure 12(*b*), the surface profile is updated to tool edge of the second pass.

When f_t is larger than $h_{\min}$, taking f_t of 2 μm as an example, the chip is formed at each engagement along the central line. There is always an interaction point between the latter tool profile and the former $h_{\min}$ profile. The surface texture needs to be updated for each engagement according to the criteria developed above, which is shown as figure 13. Then the surface roughness can be calculated from these points.

When f_t is smaller than $h_{\min}$, taking f_t of 0.2 μm as the example, the chip is not always formed during each engagement along the central line. There is no interaction point between the tool edge geometry and the minimum chip thickness bound until several engagements, shown as figure 14(*a*). The interaction happens after three engagements. The surface profile is only updated on these occasions, which

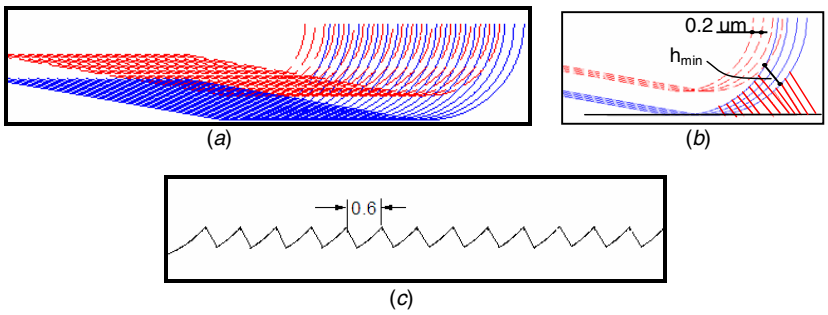

Figure 14. Schematic diagram of the surface generation when $f_t < h_{\min}$: (*a*) trajectories of the tool path and $h_{\min}$, (*b*) algorithm for the update of the surface profile and (*c*) the generated surface profile.

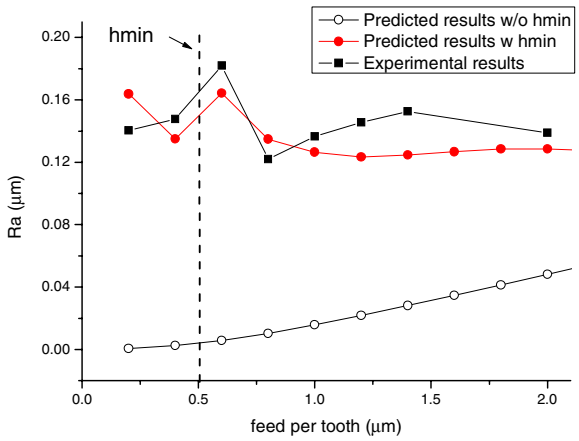

Figure 15. Comparisons of the predicted surface roughness with the experimental data.

is shown as figure 14(*b*). Figure 14(*c*) shows the generated surface profile. The period of the surface profile under this condition is 0.6 μm instead of f_t (0.2 μm) since a chip forms every three passes.

4.4. Model validation

By using the approach proposed above, the concept of $h_{\min}$ is taken into account in the trajectory-based model. In order to validate the proposed model, the experiments were performed at a spindle speed of 20 000 r min^{-1} and a DOC of 10 μm. f_t was selected to be 0.2 μm, 0.4 μm, 0.6 μm, 0.8 μm, 1 μm, 1.2 μm, 1.4 μm and 2μm, respectively. For each test, a 6 mm long channel was machined by using the same tool, which made its total cutting length as long as 48 mm. The material removal volume, which is 0.048 mm^3, satisfied the requirement of Ra_0 since the surface roughness did not vary much within ten channels (0.2 mm^3 in material removal volume) according to the tool wear experimental results seen in figure 7(*a*).

The results are shown in figure 15, in which x represents the feed per tooth of the milling process and y is surface roughness values. It is observed that the experimental data are close to the predicted results by the proposed model considering the minimum chip thickness. For the predicted results, Ra decreases when f_t is between 0.6 μm and 1.2 μm, after that there is a slight increase from 1.2 μm to 3 μm. For experimental data, Ra decreases largely when f_t increases from 0.6 μm to 0.8 μm, and after that there is an increase in trend when f_t is from 1.0 μm to 3.0 μm. In this study, the fabricated channels are all of width 0.1 mm, which makes the measurement of the surface roughness a challenging task. Considering the measurement errors, the surface roughness model based on the minimum chip thickness concept accurately predicted both the feed rate trends and the magnitude of the surface roughness for the micro-end-milling process. This fully demonstrates that the proposed model is valid and accurate.

In addition, the predicted results without considering $h_{\min}$ are also plotted in the figure to show the effect of the minimum chip thickness. The differences between the predicted results with and without considering $h_{\min}$ show the contributions of minimum chip thickness effect. It is observed that the differences are very large, especially when the feed rate is small, which indicates that the minimum chip thickness is a dominant factor responsible for the surface generation in micro-end-milling. In addition, the differences are found to decrease with the increase of the feed rate. This trend is consistent with the fact that the effect of the minimum chip thickness would be negligible when the feed rate approaches the macro level.

5. Modelling of the surface roughness considering the tool wear effect

5.1. Surface roughness degradation model calibration

According to the guideline for the surface roughness model proposed in section 3.5, the second part is the surface roughness degradation model considering the effect of the tool wear shown as equation (4). It is calibrated through regression analysis of the experimental data, in which all the seven sets of the experimental data (as shown in figure 8) were used. The coefficients C_{Ra}, m_{Ra}, n_{Ra} are calibrated to be 0.1882, 0.67 and 0.59, respectively. Therefore, the proposed model can be expressed as follows:

$$\begin{aligned} \mathrm{R}_a &= K_{\mathrm{Ra}} \cdot \mathrm{R}_{a0} \\ \mathrm{R}_{a0} &= \mathrm{R}_{a0}(f_t, h_{\min}, r_e) \\ K_{\mathrm{Ra}} &= C_{\mathrm{Ra}} \cdot V^{m_{\mathrm{Ra}}} \cdot MR^{n_{\mathrm{Ra}}} = 0.1882 V^{0.67} MR^{0.59}. \end{aligned} \tag{7}$$

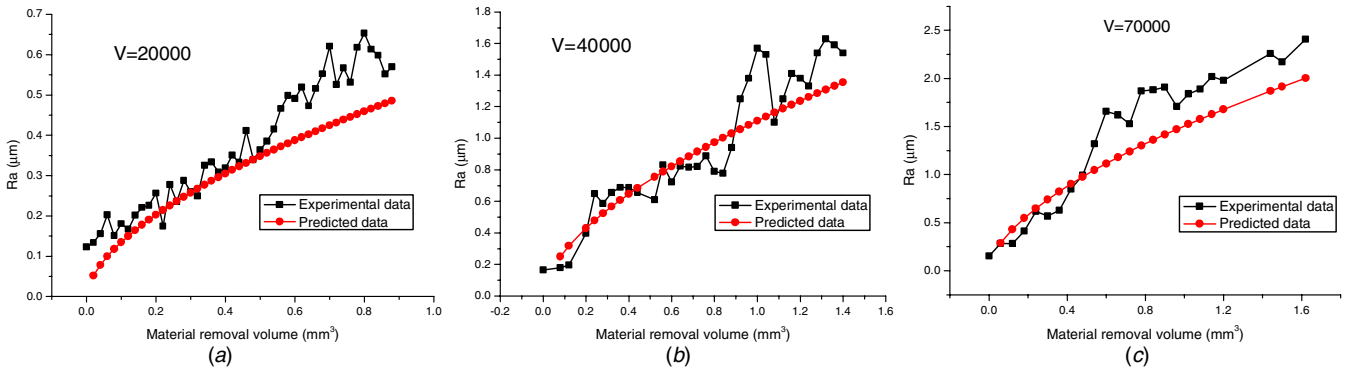

Figure 16. Validation of the surface roughness model considering the effect of the tool wear: (*a*) $V = 20\,000$ r min^{-1}, (*b*) $V = 40\,000$ r min^{-1} and (*c*) $V = 70\,000$ r min^{-1}.

5.2. Model validation

In order to examine the effectiveness of the proposed surface roughness model, the correlations between the predicted results and the experimental data were performed as shown in figure 15. In general, good agreements in both the magnitudes and trends can be observed from a comparison of the results over a wide range of cutting speeds.

Figures 16(*a*)–(*c*) show the comparison of the simulated and experimental results when the rotation speed of the spindle is 20 000, 40 000 and 70 000 r min^{-1}, respectively. As can be seen from the figures, the Ra values at the start phase of the cutting are very small, only several hundreds of nanometres, which means that the surface quality is very good. For each test at the given cutting velocity, the Ra values increase with tool wear progress. The higher the cutting speed, the quicker the surface roughness increases. The model is shown to be able to accurately predict the surface roughness over the tool life span and a wide range of machining speeds. This demonstrates that the proposed model can accurately capture the variation trend of surface roughness when tool wear progresses at different cutting speeds.

6. Conclusions

In this study, a trajectory-based surface roughness model is developed for micro-end-milling considering the effects of tool wear, minimum chip thickness and tool geometry. The proposed model is validated by micro-end-milling experiments with a miniaturized machine tool. The following conclusions can be drawn:

(1) The effect of tool wear on the surface roughness is found to be significant through the milling experiments of OFHC Copper with 0.1 mm diameter micro endmills. In some conditions, the Ra values increase several times with tool wear progress, which makes it necessary to consider the tool wear for surface roughness modelling in the micro-end-milling process.

(2) The cutting velocity and material removal volume are found to have a great influence on tool wear through the experimental analysis. The higher speed causes more rapid tool wear, which in turn makes the increases in the surface roughness much quicker. It is also observed that the depth of cut and feed per tooth have very little effect on the tool wear.

(3) The minimum chip thickness greatly affects the surface roughness in micro-end-milling. With the decrease of the feed rate, this effect is becoming much more significant, especially when the feed per tooth is close to or smaller than the minimum chip thickness.

(4) A trajectory-based surface roughness model considering the effects of tool wear, the minimum chip thickness and micro tool geometry is developed. This model accurately predicts the surface roughness variation with tool wear progress and provides means for further process design and optimization studies of the micro-end-milling process.

Acknowledgments

The support of the National Natural Science Foundation of China under grant 50575134, the National Basic Research Program of China under grant no 2005CB724100 and the Programme of Introducing Talents of Discipline to Universities under grant no B06012 is gratefully acknowledged.

References

Babin T B, Lee J M, Sutherland J and Kapoor S G 1985 A model for end milled surface topography *Proc. 13th NAMRC* pp 362–8

Bao W Y and Tansel I N 2000 Modeling micro-end-milling operations: Part III. Influence of tool wear *Int. J. Mach. Tool Manuf.* **40** 2193–211

Colding B N 2004 A predictive relationship between forces, surface finish and tool-life *CIRP Ann.* **53** 85–90

Jawaid A, Sharif S and Koksal S 2000 Evaluation of wear mechanisms of coated carbide tools when face milling titanium alloy *J. Mater. Process. Technol.* **99** 266–74

Kim C-J, Mayor J R and Ni J 2004 A static model of chip formation in microscale milling *J. Manuf. Sci. Eng.* **126** 710–8

Kline W A, Devor R E and Shareef I 1982 The prediction of surface accuracy in end milling *J. Eng. Ind.* **104** 272–8

Kolarits F M and Devries W 1989 A model of the geometry of the surface generated in end milling with variables process inputs *Mechanics of Deburring and Surface Finishing Processes* vol 38 ed J R Stango and P R Fitzpatrick (New York: ASME) pp 63–78

Lai X M, Li H T, Li C F, Ni J and Lin Z Q 2008 Modelling and analysis of meso scale milling process considering size effect, micro cutter edge radius and minimum chip thickness *Int. J. Mach. Tool Manuf.* **48** 1–14

Li C F, Lai X M, Li H T and Ni J 2007 Modeling of three-dimensional cutting forces in micro-end-milling *J. Micromech. Microeng.* **17** 671–8

Li H Z, Zeng H and Chen X Q 2006 An experimental study of tool wear and cutting force variation in the end milling of Inconel 718 with coated carbide inserts *J. Mater. Process. Technol.* **180** 296–304

Medicus K M, Davies M A, Dutterer B S, Evans C J and Fielder R S 2001 Tool wear and surface finish in high speed milling of aluminum bronze *Mach. Sci. Technol.* **5** 255–68

Melkote S N and Thangaraj A R 1994 An enhanced end milling surface texture model including the effects of radial rake and primary relief angles *J. Eng. Ind.* **116** 166–74

Rahman M, Kumar A S and Prakash J R S 2001 Micro milling of pure copper *J. Mater. Process. Technol.* **116** 39–43

Shaw M C 1995 Precision finishing *CIRP Ann.* **44** 343–8

Sinan F, Caroline M C, Matthew B, Wasserman O and Burak O 2007 An experimental investigation of micro-machinability of Copper 101 using tungsten carbide micro-endmills *Int. J. Mach. Tool Manuf.* **47** 1088–100

Sutherland J W and Babin T S 1986 The geometry of surface generated by the bottom of an endmill *Proc. 14th NAMRC* pp 202–8

Sutherland J W and Devor R E 1986 An improved method for the cutting force and surface error prediction in flexible end milling systems *J. Eng. Ind.* **108** 269–79

Tony M T, Abdel E B and Guven Y S 1992 Tool wear modeling through an analytic mechanistic model of milling processes *Wear* **154** 287–304

Vogler M P, Devor R E and Kapoor S G 2003 Microstructure-level force prediction model for micro-milling of multi-phase materials *J. Manuf. Sci. Eng.* **125** 202–9

Vogler M P, Devor R E and Kapoor S G 2004 On the modeling and analysis of machining performance in micro endmilling: Part I. Surface generation *J. Manuf. Sci. Eng.* **126** 684–93

Weule H, Huntrup V and Tritschler H 2001 Micro cutting of steel to meet new requirements in miniaturization *CIRP Ann.* **50** 61–4

Yuan Z J, Zhou M and Dong S 1996 Effect of diamond tool sharpness on minimum cutting thickness and cutting surface integrity in ultraprecision machining *J. Mater. Process. Technol.* **62** 327–30